NATIONAL AERONAUTICS AND SPACE ADMINISTRATION
GODDARD SPACE FLIGHT CENTER
Greenbelt, Maryland

August 1967

GCA CORPORATION
GCA TECHNOLOGY DIVISION
Bedford, Massachusetts

SODIUM VAPOR EXPERIMENT

Quarterly Progress Report No. 8

Covering the Period

1 April - June 1967

Prepared under Contract NAS5-3970

TABLE OF CONTENTS

I. INTRODUCTION

The purpose of this contract is to investigate the dynamics of the upper atmosphere through analysis of the motion of sodium vapor trails ejected from sounding rockets. Data are taken photographically from several widely separated sites. Triangulation is used to determine winds from the rate of motion of the trail, and densitometry measurements determine the growth rate and small-scale structure of the trail. Complete descriptions of the experimental and analytical methods are given in reports covering NASA contracts NAS5-215 and NAS2-396. Theoretical studies of the dynamics of the upper atmosphere are directed toward formulation of models based on the observations. The first series of rocket firings occurred during November 1964 from Wallops Island and simultaneously from a ship at selected distances from Wallops Island. The objective of the series was to investigate the variation of the vertical wind structure at two places separated by different distances.

The results of the first series were seriously limited by vaporizer malfunction, but one set of trails separated by 180 km showed the winds to differ significantly above 120 km. Previous analysis of several up and down trails separated by a distance of about 50 km have shown no wind variations over that distance. Continuation of the study of horizontal variation of the vertical wind profile was an objective of a series of flights from Wallops Island during June 1965. Two vapor trails were ejected from rockets fired nearly simultaneously on different azimuths during the evening twilight of 22 June and the morning of 23 June. A fifth rocket ejected a trail of TMA at 2300 EST on 22 June to allow observations of the time variations of the winds.

The spatial separation of the simultaneous trails in June was not large and the differences in the wind profiles were small. The evening trails were separated by only 25 km, and the wind speed around 100 km was only about 30 m/sec. The trail separation and wind speed of the morning trails were greater than those of the evening trails. The TMA trail, because of poor rocket performance, did not reach the predicted altitude and faded very quickly, causing some loss of data in the 100 to 125 km region and reduced the accuracy of the data below that height. Thus, the information on spatial variations is limited. Much more information was obtained from the time-space trails. The low wind speeds during evening twilight had increased by a factor of 2 to 3 by 2300 EST (about 3 hours later) and the familiar spiral pattern had begun to form. The clockwise spiral was even more apparent over much of the height region by morning twilight and the whole pattern had been continually rotated through the night, as has been previously observed in other time sequences in January and July 1964. The observations should be more closely spaced in order that the exact nature of the changes may be determined. Such closely spaced observations were the purpose of the series of firings at Wallops Island in January 1966.

During the night of 17-18 January 1966, five vapor trail payloads were successfully launched from Wallops Island. This series showed that observations spaced an hour or two apart provide much information concerning the manner in which the winds vary. Some of the initial observations were discussed in the Quarterly Report covering the period 1 January 1966 - 31 March 1966. It was shown that the large scale spiral pattern collapsed into an irregular low speed pattern in about 6 hours and that the entire pattern moved slowly downward.

Five vapor trails were successfully launched from Wallops Island during the night of 16-17 July 1966. Again it appears that a part of a large scale cyclic pattern was observed during the 8-hour period in which the firings occurred. The downward motion of the entire profile which was observed in the January 1966 series of trails was also present in the July series. However, this effect was not clearly defined in the last two profiles of the series and effects due to sunrise at the observed altitude could not be positively identified. A discussion of the objectives of this series and plans for repeating it are given in Section II of this report.

During the night of 31 January - 1 February 1967 a series of six vapor trails were successfully ejected from Nike Apache rockets fired at Ft. Churchill, Canada. The results from five of these were discussed in the previous quarterly report. The wind profile from the other trail is contained in Section III of this report in which general methods of data analysis are also discussed.

Recent disclosures by other investigators utilizing the vapor trail method have raised the question of accuracy and application of the method. Section IV of this report discusses these questions and presents an analytical description of the method of obtaining winds from a vapor trail.

II. DISCUSSION OF SEQUENTIAL VAPOR TRAILS

Two series of sequential vapor trails were conducted at Wallops Island during 1966. Five trails were spaced throughout the night of 17-18 January 1966. Four of the trails were spaced between evening twilight and midnight, a period of about 6 hours. At the beginning of the period the winds formed the familiar large spiral pattern. By midnight, the wind speed had decreased greatly, and the winds formed an irregular pattern. The decrease in speed did not take place isotropically. The initial large spiral first collapsed into a narrow ellipse in which wind components directed toward the northeast and southwest were greatly diminished, whereas the wind components directed toward the northwest and southeast remained high. Then these components decreased as well, leading to the small, irregular pattern.

The data from these observations allowed the following preliminary conclusions:

1. The large spiral pattern collapsed to a small irregular one in

six hours, suggesting that the collapse was possibly due to a semi-diurnal tidal oscillation.

2. The entire wind profile appeared to move slowly downward throughout the period. The rate of downward motion was about 3 meters/sec. at 130 km, and about 1 meter/sec. at 110 km. This downward motion probably represents a "phase motion," i.e. the motion of a point of constant phase of the velocity field. In this case the direction of the motion (downward) is expected to be the same at all times. On the other hand, the observed motion may represent an actual mass motion, in which case it must reverse itself at some time. If this motion is assumed to be periodic, the observed motions can be described by the empirical equation

$$w = w_o \, e^{kz} \cos \frac{2\pi}{T} (t-\delta)$$

where w = upward velocity

$w_o = 5.64 \times 10^{-3}$ meter/sec

$k = 0.0482$/km

$T = 24$ hours

$\delta = 9.28$ hours.

The numerical values of the parameters were determined from the data. The value of δ implies that the times at which the motion reverses direction are 3.28 hours and 15.28 hours. If the observed motion is indeed a mass motion, then these times are consistent with the calculation of Harris and Priester. They found the times of maximum and minimum density to be at 4 hours and 14 hours respectively. It must be noted that their calculation applies to the upper thermosphere and the exosphere, whereas the reported observations were from the lower thermosphere.

3. Much of the small-scale structure on the wind profiles persisted throughout the period of observation and moved downward together with the large features.

A second series of closely spaced trails was observed during the night of 16-17 July, 1966. Four of the trails were spaced between midnight and morning twilight. Aside from the continued observation of the temporal variation of the winds, this series had two specific objectives. The first was to determine whether the downward motion of features on the wind profile continued until morning twilight. The second was to investigate an abrupt change in the wind patterns at sunrise, as reported from measurements of the motion of ionized meteor trails. The variation of the wind pattern during the night was similar to that of 17-18 January in some respects. The first pattern of the series at evening twilight had some of the character of the spiral pattern, but it was not completely formed. By midnight the pattern had changed into one in which the winds were primarily East-West. The North-South component had continued to decrease up to 0145 EST. Between that time and 0325 EST, the time of the next observation, the North-South component had increased considerably. It can not be determined if the East-West wind collapsed to form a small irregular pattern during the period between 0145 and 0325 EST. At 0408, the pattern from the morning twilight trail again showed some of the spiral character and was very similar to that of the evening twilight. Thus again a large part of a cyclic pattern may have been observed during the eight-hour period. The apparent downward motion of the entire wind pattern was observed during part of the period but was not uniquely determined during the last two measurements due to ambiguities in the determination of corresponding features on the successive profiles. This is unfortunate since a continuation of the downward motion would strongly suggest that the observation concerned the phase velocity of a slowly propagating wave. A reversal of the direction of the vertical motion might indicate a mass motion produced by a cooling and heating process.

A similar uncertainty is attached to the twilight effect which was suggested by the meteor data. There is a relatively large change in the wind pattern between the 0325 and 0408 profiles: The height interval measured at 0325 was in complete darkness at that time. This same region was completely illuminated at 0408. Thus some of the change during that period could be attributed to an effect associated with sunrise. However, a normal cyclic effect was also apparently in progress, i.e. the formation of a large spiral pattern. The change could also be associated with this effect. It is of interest to compare the energy associated with the winds during this period. Plots of the kinetic energy density $(1/2\ \rho V^2)$

as a function of height are given in Figures 1-2. It is seen that in all except the first profile (14:292, obtained at midnight) the greatest wind energy is below 100 km and increases rapidly after midnight. The increase in total energy does not seem to be greater during the twilight period. There seems to be an upward motion of the features in the energy profiles during the twilight period, but the question of an abrupt twilight effect is not answered.

Since both of the special objectives of the series were not clearly decided, it is recommended that the series be repeated. The objectives would be the same as previously outlined, i.e. to study the temporal changes in the high-altitude winds, and specifically to investigate the apparent vertical drift of the profile to determine if such motion is due to the phase velocity of a traveling wave, or whether it is associated with actual mass motion (probably due to local cooling and heating). Also, the effect of sunrise on the wind profile will be observed to determine if an unusually large energy input is introduced at this time.

Specifically it is proposed that a vapor trail to measure the winds in the region 90 to 135 km be ejected by rocket at the following times: evening twilight, midnight, approximately 80 minutes before sunrise at 100 km, approximately 40 minutes before sunrise at 100 km, and during morning twilight, when the 100 km region is fully illuminated. This schedule will allow the determination of the long-period changes in the pattern throughout the night, and also allow a detailed observation of the changes occurring just prior to and during sunrise.

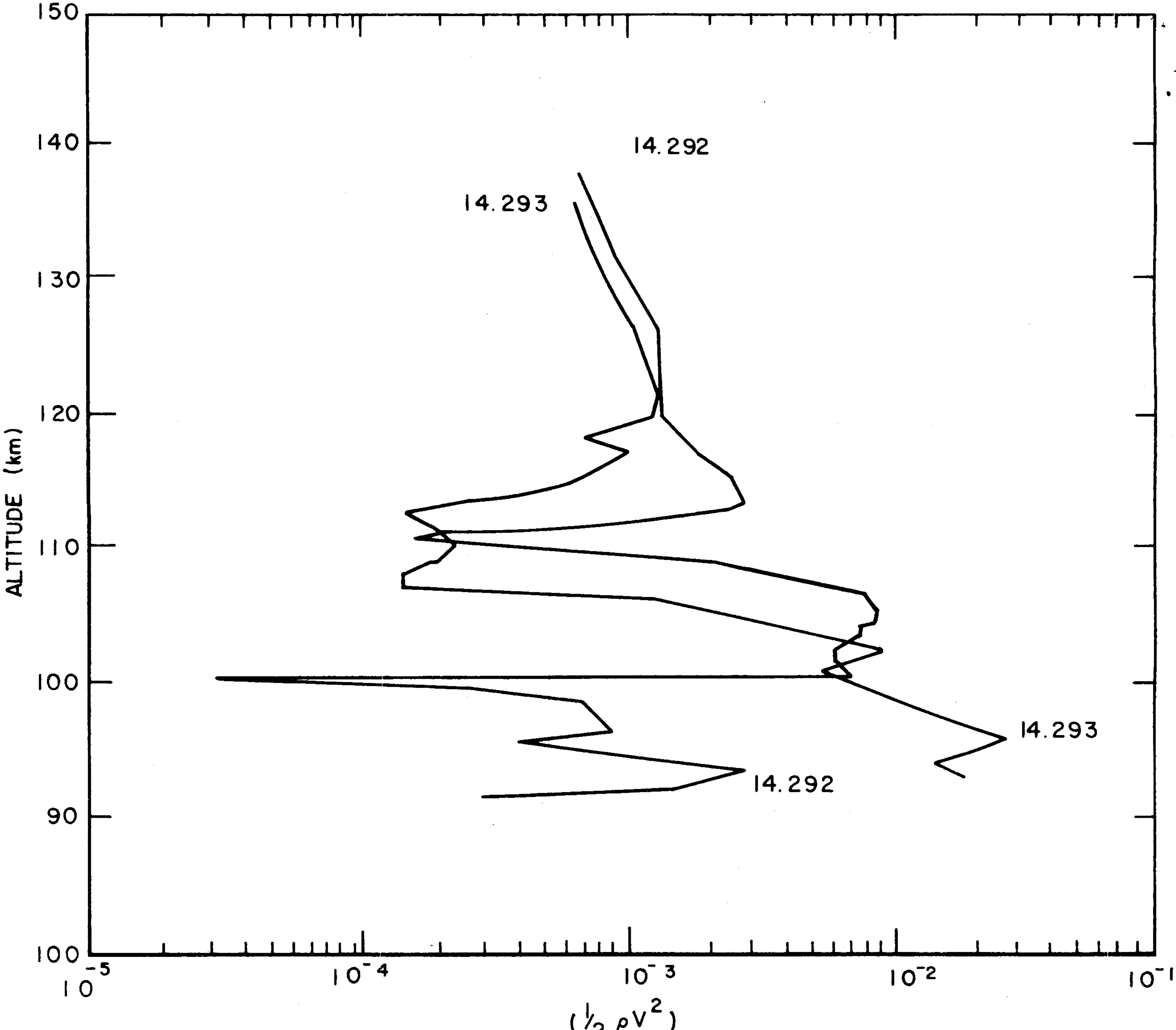

Figure 1. Kinetic energy density vs height.

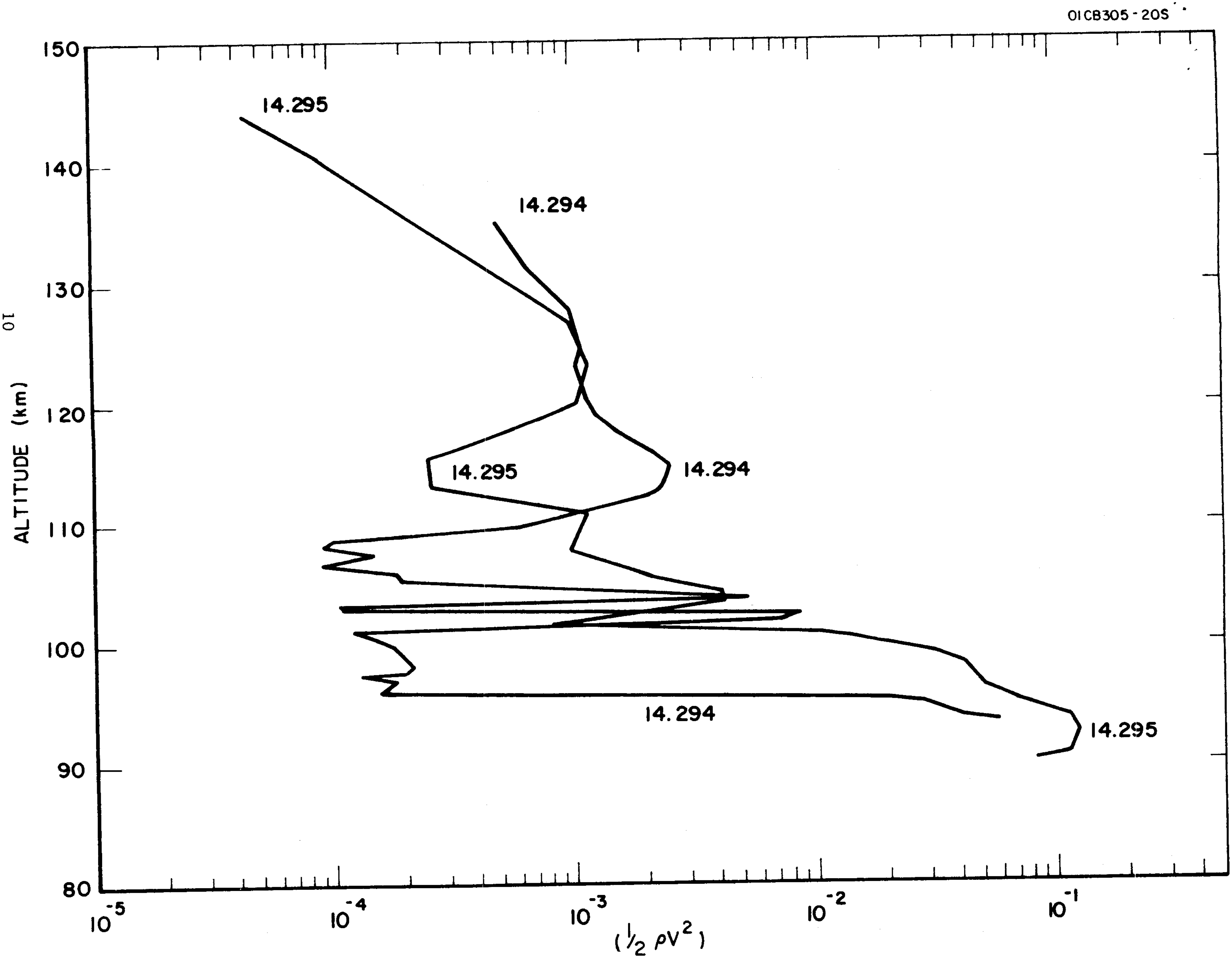

Figure 2. Kinetic energy density vs height.

Much of the effort during the reporting period was directed toward construction of two akali vapor and four TMA payloads and preparation of photographic equipment. Camera sites will be activated at the usual locations, Dover A.F.B., Andrews A.F.B., Camp A. P. Hill, and Dam Neck Naval Training Station. Each site will have the following equipment, (1) standard 70 mm cameras, (2) fast f/1.5 70 mm cameras for dim night trails, and (3) K-24 cameras with 20 in. lenses for recording small scale structure.

Due to an unusual weather condition which caused continuous cloudiness over the Eastern Seaboard, the firings did not take place until 8 August during the final preparation of this report. All flights were successful and will be reported in detail in the next report.

III. WIND DATA AND ANALYSIS

The wind data from all but one of the trails in Ft. Churchill during January 1967 were included in the last report. The data from the remaining trail (NASA 14.310) is given in Figure 3. The general features of the other five wind profiles were discussed in the last report. NASA 14.310, the first rocket of the series, was fired at 1720 CST, almost 2 hours before the second firing. Thus the series covered the period 1720 CST 31 January to 0524 CST, 1 February, a total of 10 hours. Throughout the period the general pattern changes slowly suggesting a half period of the order of 6 hours. More detailed analysis of the wind data is being done in two ways: (1) Detailed Analysis of

Figure 3. Hodograph for trail from NASA 14.310.

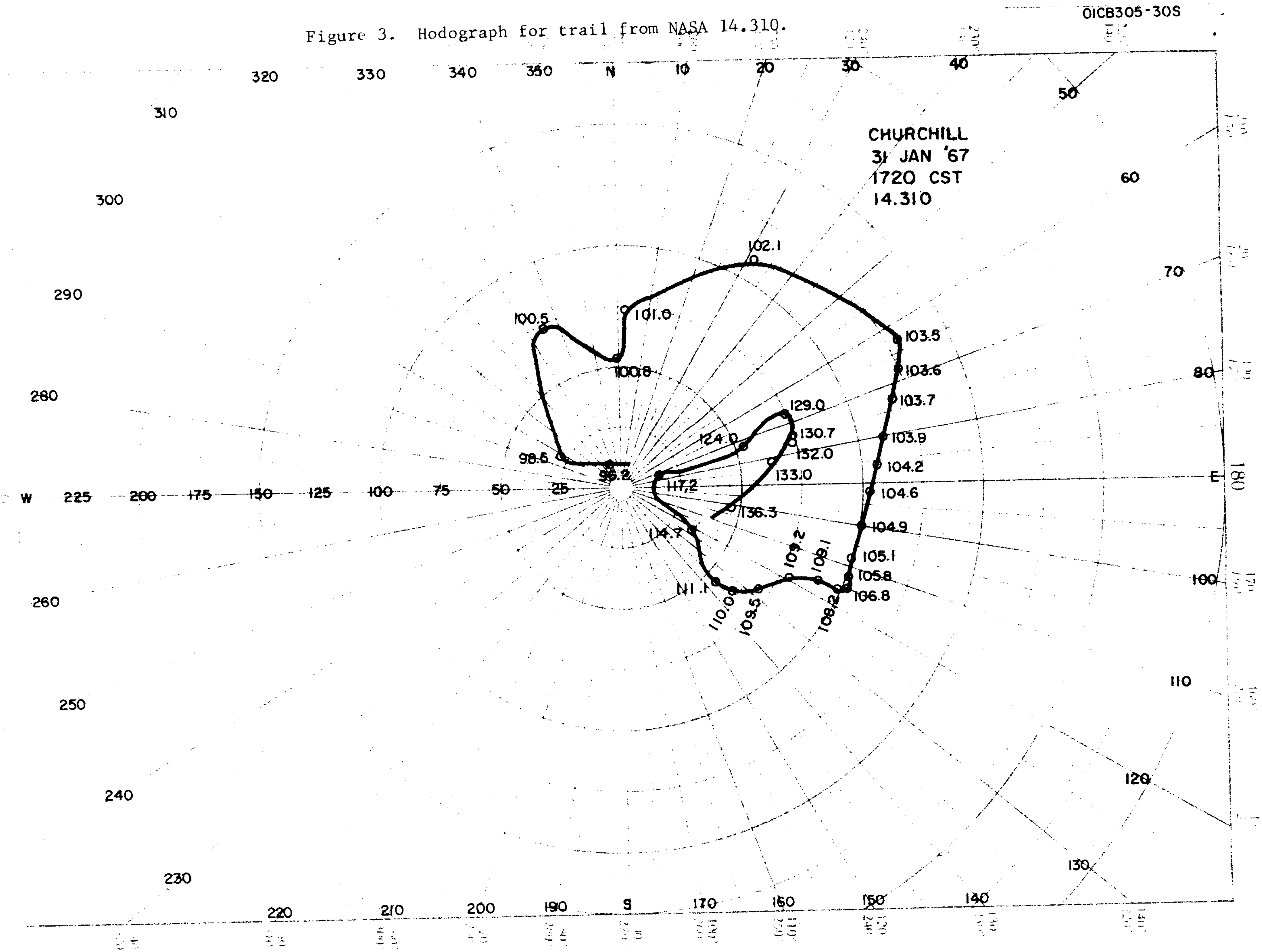

of Time Series, and (2) Statistical Analysis.

(1) Detailed Analysis of Time Series

A time series provides a set of measurements closely spaced in time. Such measurements make possible the quantitative evaluation of the temporal rate of change of the wind velocity. That part of the temporal change due to the Coriolis force can be calculated and subtracted from the observed change. The residual change of velocity must then be accounted for by the pressure gradients and by the non-linear terms in the equations of motion. The largest of the non-linear terms is the product of the vertical wind, w, and the vertical derivative of the wind velocity, $\partial\vec{V}/\partial z$. The vertical derivative can be calculated from the data, but the vertical wind w is too small to be measurable. Nevertheless, it is useful to compare the profiles of the time derivative and the vertical derivative of the wind velocity. A close similarity between these two profiles would confirm the essential non-linearity of the wind system at these heights.

Distinguishable features of the wind profile that are identifiable in consecutive measurements of a time series are used to provide a semi-quantitative evaluation of the vertical drift of these features. Most probably, this vertical drift represents a phase motion, but the possibility that it represents a mass motion cannot be excluded at this time.

(2) Statistical Analysis

A computer program has been written to evaluate, tabulate and average various quantities of interest. Among these are the square of the wind velocity, which is proportional to the kinetic energy; the square of the vertical derivative of the wind velocity, which is proportional to the rate of dissipation of kinetic energy; the second vertical derivative of the wind velocity, and the curvature at each point of a wind hodograph. One or the other of the last two quantities is related quantitatively to the presence of "corners" in the wind hodograph.

It is useful to represent winds as functions not of the real height z, but of the "normalized height" ζ, defined by the equation

$$\zeta = \int_{zo}^{z} \frac{dz'}{H(z')}$$

where H is the scale height. One can then infer vertical wavelengths from the correlation function

$$C_1 (h) = \frac{\int d\zeta \; V(\zeta) \; V(\zeta+h)}{\int d\zeta \; V(\zeta)^2}$$

It is also possible to infer vertical drift velocities in a time series from the correlation function

$$C_2\ (t_1,\ t_2,\ h) = \frac{\int d\zeta\ V\ (t_1, \zeta)\ V\ (t_2,\ \zeta + h)}{\left[\int d\zeta\ V\ (t_1,\ \zeta)^2 \int d\zeta'\ V\ (t_2,\ \zeta')^2\right]^{\frac{1}{2}}}$$

Unfortunately the scale height is not a known quantity. It varies with latitude, local time, and with the solar cycle, and these variations are not at present known. Thus the use of "normalized heights" determined from a standard atmosphere runs the risk of introducing spurious effects. Nevertheless, the calculation will be made on the basis of the existing information, and revised as new information is made available.

IV. ACCURACY OF THE VAPOR TRAIL METHOD

During May, Dr. E. Constantinides and J. F. Bedinger attended the A.M.S. Symposium on the upper atmosphere in Miami and participated in panel discussions. Although it was not included in the agenda, the accuracy of the vapor trail method became an important issue when reports of observations of vertical winds and turbulent structure were discussed. It was pointed out that usually vapor trails had small irregular structure and sharp features, (shears, corners) which could be positively identified for extended times and thus upper limits to vertical velocities and irregular motions could be determined. It is usually admitted by most investigators using the vapor trail method that a point on the trail around 100 km can be determined to within 0.1 km. The equivalent velocity error, ΔV_{σ}, that results from this uncertainty in position determination at two times separated by Δt, is

$$\Delta V_{\sigma} = 2 \times 100/\Delta T, \text{ meters/sec.}$$

Usually observations may be made for several minutes, and assuming $\Delta t = 200$ sec., ΔV_{ϵ} is less than 1 m/sec. This is the upper limit which was placed on the vertical velocities at 100 km by J. Bedinger at the A.M.S. meeting. It is obvious that if Δt is smaller, say 20 sec., the ΔV_{ϵ} is proportionately larger, 10 m/sec. Lower limits for ΔV_{ϵ} for short observation times may usually be obtained by a comparison of the relative positions of several identifiable points on the successive photographs from the same observing sites.

In order to assist in evaluation by those people not actively involved in vapor trail measurements an analytical description of the method was prepared and included as an appendix to a paper being submitted for publication in J.G.R.. This description is included in an appendix to this report for the same reason.

V. PLANS FOR THE NEXT REPORT PERIOD

Processing and reduction of data from the August series of vapor trails at Wallops Island will begin during the next quarter. Analysis of wind data as discussed in Section III of this report will continue.

APPENDIX. WIND MEASUREMENTS BY THE PHOTOGRAPHIC METHOD.

Let $\underline{V}(\underline{x},t)$ denote the velocity of a particular fluid element in a vapor trail. The components of $\underline{x}$ are Lagrangian coordinates, the fluid element being identified by its position $\underline{x}_0$ at time t=0 when it lies on the rocket trajectory. Thus each element of the trail has its own time scale.

For the time intervals and horizontal displacements contemplated in the following discussion we may, in a first approximation, neglect both the explicit time dependence of $\underline{V}$ and its dependence on the horizontal coordinates x, y, and write $\underline{V} = \underline{V}\left[z\ (t)\right]$.

The displacement of an element is given by

$$\underline{x} - \underline{x}_0 = \int_0^t \underline{V}\left[z(t')\right] dt' \tag{A.1}$$

For sufficiently small vertical displacements, we may neglect variations of V_z, so that

$$z - z_0 \simeq V_{z0}t \simeq V_z t \tag{A.2}$$

The horizontal component of $\underline{V}$ is accordingly given by

$$\underline{V}_h(z) = \underline{V}_{h0} + V_{z0}t\left(\frac{d\underline{V}_h}{dz}\right)_0 \tag{A.3}$$

whence it follows that

$$\underline{x}_h - \underline{x}_{h0} = t\underline{V}_{h0} + \tfrac{1}{2}t^2 V_{z0} \left(\frac{d\underline{V}_h}{dz}\right)_0 = t\underline{V}_h - \tfrac{1}{2}t^2 V_z \frac{d\underline{V}_h}{dz} \qquad \text{(A.4)}$$

The left side of (A.4) represents the horizontal displacement of an element of the trail. Since the trail is continuous, however, individual elements cannot in general be identified, so that the displacement given by (A.4) is not directly measurable. What can be measured is the displacement $\underline{D}(h,t)$ at a given height h. $\underline{D}$ represents the position vector of a point on the trail drawn from a point at the same height on the rocket trajectory. From the fact that the Eulerian displacement $\underline{D}$, the Lagrangian displacement $(\underline{x}(h)-\underline{x}(h_0))$, and a section of the rocket trajectory between the heights z_0 and $z(t) = h$ form a triangle, it follows that

$$\underline{D}\,(h,t) = (\underline{x} - \underline{x}_{h0}) - t\, V_z \cot\alpha\, \hat{\underline{k}} \qquad \text{(A.5)}$$

where α is the elevation angle of the rocket trajectory at the height in question and $\underline{k}$ is a horizontal unit vector lying in the vertical plane through the rocket trajectory. From equations (A.4) and (A.5) we have

$$\underline{D}\,(h,t) = t(\underline{V}_h - V_z \cot\alpha\, \hat{\underline{k}} - \tfrac{1}{2}t^2 V_z \frac{d\underline{V}_h}{dz}) \qquad \text{(A.6)}$$

The apparent horizontal velocity may be defined as the displacement $\underline{D}$ divided by the elapsed time t. It is given by

$$\underline{V}_h^{app} = \underline{D}/t = (\underline{V}_h - V_z \underline{k} \cot\alpha) - \tfrac{1}{2} t V_z \frac{d\underline{V}_h}{dz} \qquad (A.7)$$

$\underline{V}_h^{app}$ reduces to the true horizontal velocity $\underline{V}_h$ when $V_z = 0$.

The measured displacement $\underline{D}^{meas}$ may differ significantly from the actual displacement $\underline{D}$. Now, if t is given, the functions $D^{meas}(h)$ and $\underline{D}(h)$ describe two curves in space. In general, the two curves may be connected by an infinity of coordinate transformations, each describing a distinct mapping of one curve onto the other. Symbolically, if we write

$$\underline{D}^{meas} = \underline{D}(h + \eta) + \underline{\Delta} \; . \qquad (A.8)$$

there are in general infinitely many ways of choosing the functions $\eta(h)$ and $\underline{\Delta}(h)$.

In particular cases, however, the ambiguity can be resolved. For example, suppose that the curve $\underline{D}(h)$ has a cusp. If the curve $\underline{D}^{meas}$ has a corresponding feature, then for this feature the values of η and $\underline{\Delta}(h)$ will have specified values at two heights, and considerations of continuity serve in practice to restrict the values they can assume between these heights.

A detailed consideration of the errors of measurement may also serve to restrict the functions $\eta(h)$ and $\underline{\Delta}(h)$. For example, the geometrical configuration of the observing sites and the trail may permit horizontal coordinates to be measured with greater accuracy than heights.

On expanding the right side of (A.8) to first order, we obtain, with the help of(A.6)

$$\underline{D}^{meas} = \underline{D} + \eta t \frac{d\underline{V}_h}{dz} + \underline{\Delta} \tag{A.9}$$

which shows that height errors affect the measured displacement differently from errors in the assignment of horizontal coordinates.

The measured horizontal velocity is given by

$$\underline{V}_h^{meas} = \frac{\underline{D}^{meas}}{t} \tag{A.10}$$

Inserting (A.7) and (A.9) into this formula, we obtain

$$\underline{V}_h^{meas} = (\underline{V}_h - V_z \cot\alpha\, \hat{\underline{k}} + \eta \frac{d\underline{V}_h}{dz}) - \tfrac{1}{2}\, t\, V_z \frac{d\underline{V}_h}{dz} + t^{-1}\, \underline{\Delta} \tag{A.11a}$$

or

$$\underline{V}_h^{meas} = (\underline{V}_h - V_z \cot\alpha\, \hat{\underline{k}}) + (\eta - \tfrac{1}{2}\, t\, V_z) \frac{d\underline{V}_h}{dz} + t^{-1}\, \underline{\Delta}. \tag{A.11b}$$

It is convenient to introduce the quantity

$$\underline{U} = \underline{V}_h - V_z \cot\alpha \, \underline{k}. \tag{A.12}$$

To first order we may then write equation (A.11b) in the form

$$\underline{V}_h^{meas} = \underline{U} + (\eta - \tfrac{1}{2} tV_z) \frac{d\underline{U}}{dz} + t^{-1} \underline{\Delta} \tag{A.13a}$$

$$= \underline{U}(h + \eta - \tfrac{1}{2} tV_z) + t^{-1} \underline{\Delta} \tag{A.13b}$$

if $\underline{\Delta}$ is sufficiently small or if t is sufficiently large, the last term on the right side of equation (A.13b) may be neglected, and the resulting equation can then be written in the form

$$\underline{V}_h^{meas}(h + \Delta h) = \underline{U}(h) \tag{A.14}$$

where

$$\Delta h = -\eta + \tfrac{1}{2} tV_z. \tag{A.15}$$

Equation (A.14) is convenient for the analysis of observations. Given a set of n measured profiles $\underline{V}_h^{meas}(h, t_i)$, i = 1, 2,..., n, we can at every height evaluate n-1 linearly independent combinations of the n increments Δh. If the number of profiles is not too small, it may be a good approximation to assume that the average value of Δh vanishes at all heights; in this way we arrive at an approximation to the function $\underline{U}(h)$. If, now, it is possible to separate the two terms on the right side of equation (A.15) by examining the way in which Δh varies with time at a given level, we can obtain V_z as a function of height, and then, from equation (A.12), $\underline{V}_h$. This method has been used successfully to measure vertical winds in a few cases.